RESEARCH

Synthesis and characterization of silica nanoparticles from rice husk and their effects on physiology of rice under salt stress

Preeyanuch Larkunthod[1], Jakkree Boonlakhorn[2], Payu Pansarakham[3], Paweena Pongdontri[3], Prasit Thongbai[2], and Piyada Theerakulpisut[1*]

[1]Khon Kaen University, Salt-Tolerant Rice Research Group, Faculty of Science, Department of Biology, Mittraphap Road, Khon Kaen 40002, Thailand. *Corresponding author (piythe@kku.ac.th).
[2]Khon Kaen University, Faculty of Science, Department of Physics, Mittraphap Road, Khon Kaen 40002, Thailand.
[3]Khon Kaen University, Faculty of Science, Department of Biochemistry, Mittraphap Road, Khon Kaen 40002, Thailand.

Received: 19 December 2021; Accepted: 8 March 2022; doi:10.4067/S0718-58392022000300412

ABSTRACT

Silicon (Si) is considered a beneficial element for rice (*Oryza sativa* L.) The objective of this work was to investigate the effects of Si in the form of nanoparticles on growth and physiology of rice under salt stress. Silica nanoparticles (SNPs) were synthesized from rice husk by sol-gel method. The prepared SNPs powders were agglomerated in semi-spherical nano-sized particles with diameters in the range of 60-135 nm. Three rice cultivars namely 'Pokkali', 'KDML105' and 'IR29' were grown for 30 d in plastic pots, and then divided into four groups i.e., control, SNPs, NaCl and NaCl + SNPs. Foliar spray of 120 mg L^{-1} SNPs was given to the SNPs and NaCl + SNPs groups for 4 d. After that the plants in NaCl and NaCl + SNPs groups were exposed to 150 mM NaCl for 17 d. The salt-stressed plants suffered significant reductions in biomass, net photosynthesis rate (P_N), and maximal quantum efficiency of photosystem II (PSII) photochemistry (F_v/F_m) while three stress indicators (malondialdehyde, hydrogen peroxide [H_2O_2] and proline) considerably increased. The SNPs mitigated the adverse effects of salt stress by increasing P_N (18% to 116% increase) and lowering H_2O_2 (8% to 31% reduction) in all cultivars, compared with the values under salt stress, while proline was reduced by 7% in 'KDML105' and 19% in 'IR29'. The H_2O_2 content was regulated by the increased activities of antioxidant enzymes, notably catalase, peroxidase and ascorbate peroxidase. The application method and concentrations of SNPs used for rice plants under stress should be further optimized for the highest benefit of growth and yield in the field conditions.

Key words: Antioxidant enzymes, efficiency of PSII, malondialdehyde, net photosynthesis rate, *Oryza sativa*, proline, rice, salt stress, silica nanoparticles.

INTRODUCTION

Silicon (Si) is considered a non-essential element for growth and development of plants, and most plants can grow normally in its absence (Zhu and Gong, 2014). Nevertheless, in some plants especially graminaceous crops such as rice, wheat and sugar cane, Si is regarded as a beneficial element which enhances plant vigor, increases tolerance to abiotic stress (drought, salinity, heat, and heavy metal stress), and offers great protection against diseases and pest (Zargar et al., 2019). Silicon is absorbed by plant roots in the form of silicic acid ($Si(OH)_4$), transported via xylem to stems and leaves where Si benefits plants by offering physical and mechanical protection by deposition of SiO_2 in cell walls, and modifying a range of biochemical, physiological, and metabolic processes (Luyckx et al., 2017). For rice, Cuong et al. (2017) reported that increasing levels of Si fertilizer supplements resulted in increasing growth and yields in the field

condition. The optimum dosage of 329 kg ha^{-1} of Si fertilizer produced 23% higher grain yield compared with the control fields without Si supplements. Application of Si fertilizer also alleviated adverse effects and promoted rice growth under drought and heat stress (Agarie et al., 1998) and salt stress (Abdel-Haliem et al., 2017). The Si application was reported to alleviate deleterious effects of salt stress by (1) decreasing Na^+ and increasing K^+ concentration in cytoplasm by activating ion transporter proteins in plasma membrane and tonoplast, (2) diluting Na^+ concentration in the cells by increasing water content, (3) decreasing oxidative damage by modulating plant antioxidant defense systems, (4) regulating biosynthesis of compatible solutes, (5) promoting cellular extension growth by reducing lignification in the cell wall, and (6) regulating levels of abscisic acid and polyamine which results in enhancing stress tolerance (Zhu and Gong, 2014).

Rice (*Oryza sativa* L.) is known as Si accumulator, and it was estimated that 20 kg ha^{-1} SiO_2 is removed from the soils for every 100 kg harvested rice grains (Ma et al., 2002). With intensive rice cultivation, enormous amount of Si was removed to the point that it has become a limiting factor for rice production in some areas, and farmers need to replenish Si by applying Si fertilizers. The recommended dose, in rice fields, of commercial Si fertilizers (commonly available in the forms of calcium metasilicate, potassium silicate, sodium silicate, and sugarcane bagasse) was approximately 1-2 t ha^{-1} (Savant et al., 1996; Liu et al., 2009) which added a substantial production cost for poor farmers. Recent reports presented that Si in the form of nanoparticles of SiO_2 can be applied to plants at considerably lower doses compared to the commercial Si fertilizer (Abdel-Haliem et al., 2017; Félix Alvarez et al., 2018). Moreover, low-cost production of silica nanoparticles (SNPs) through appropriate calcination process could be effectively prepared from agricultural waste such as rice husk, which contained about 20% of SiO_2 (Huang et al., 2019). These SNPs particles are inert, non-toxic, and has a porous structure with a nanometer scale and a high surface area (Pal et al., 2020). Due to their unique physical and chemical properties, SNPs exhibit great potential in agriculture because they are more readily absorbed due to nanoscale size and work more effectively than the bulk Si compounds in commercial fertilizers in promoting plant growth and alleviating different abiotic stresses (Rastogi et al., 2019).

Salinity is one of the main abiotic stresses which threatens rice production at varying stages from seed germination, seedling, vegetative through to reproductive growth (Farid et al., 2021). In Thailand, rice is most widely cultivated in the northeast of the country where soils are affected by salinity, causing low yields compared to other geographical locations (Kanawapee et al., 2012). Utilizing the outstanding properties of SNPs, either as soil amendments or foliar application, is an interesting approach to explore for enhancement of rice growth and yield in salt-affected soils. The objectives of this study were to synthesize SNPs from rice husk; to characterize the morphology, structure, and optical properties of the obtained SNPs; and to investigate the effects of foliar application of SNPs on growth and physiological parameters under salt stress of three rice cultivars differing in salt tolerance level.

MATERIALS AND METHODS

The collected rice (*Oryza sativa* L.) husks were first washed with tap water to remove dirt and then dried in a hot air oven (UN110, Memmert, Schwabach, Germany) at 70 °C for 24 h. After moisture removal, it was calcined at 900 °C for 7 h in a muffle furnace (CHY-M1215, Henan Chengyi Equipment Science and Technology, Zhengzhou, China).

Synthesis of silica nanoparticles from rice husks

Silica extracted from rice husk (5 g) was dispersed in 500 mL 0.5 M NaOH aqueous solution and heated at 100 °C for 4 h. The solution obtained was filtered using Whatman No. 1 filter paper to remove the nonreactive impurities. The transparent filtrate of sodium silicate solution was allowed to cool at room temperature and titrated with 10% H_2SO_4 to pH 7, then left for 24 h to allow the silica gel to precipitate slowly. The formed gel was washed with deionized (DI) water and centrifuged in a refrigerated benchtop centrifuge (Velocity 18R, Dynamica, Livingston, UK) at 12000 rpm to sediment the gel. The clean silica gel was freeze-dried overnight to remove water using a freeze dryer (Scan Speed 40, LaboGene, Lillerød, Denmark). The silica nanoparticles (SNPs) product (Figure 1) was placed in a vacuum desiccator for further analysis.

Figure 1. Schematic illustration of the process of silica nanoparticles (SNPs) synthesis from rice husks.

Characterization of SNPs

The crystalline structure of the produced SNPs was examined using an X-ray diffractometer (XRD) (Empyrean, Malvern Panalytical, Malvern, UK). The XRD spectra were collected in a 2θ range of 10°-60° using a step increase of 0.02°/point. The morphology and elemental compositions of the SNPs were examined by field emission scanning electron microscopy (FE-SEM) (Helios NanoLab G3 CX, FEI Company, Hillsboro, Oregon, USA) coupled with the energy-dispersive X-ray spectroscopy (EDS) technique. Fourier transform infrared spectroscopy (FT-IR) was used to examine chemical bonds in molecules of samples using the FT-IR spectrometer (Tensor 27, Bruker, Billerica, Massachusetts, USA). Using the KBr pellet method, data for FT-IR analysis were collected in the wavelength range of 4000-400 cm^{-1}.

Effect of SNPs foliar application on growth, photosynthesis and biochemical characteristics of rice under NaCl stress

Plant materials and growth conditions. Three rice cultivars with different levels of salt tolerance namely 'Pokkali' (tolerant), 'KDML105' (moderately sensitive), and 'IR29' (highly sensitive) (Kanawapee et al., 2012) were included in this study. Seeds were surface sterilized by soaking in 10% v/v sodium hypochlorite solution for 15 min and washed several times with sterile distilled water. Seeds were then germinated on filter paper. Subsequently, four germinated seedlings (4-d-old) were then transferred to each plastic pot filled with 4 kg paddy soils. The rice plants were grown in the pots flooded with tap water to 3 cm above the soil surface in the greenhouse at the Faculty of Agriculture, Khon Kaen University, Khon Kaen, Thailand. When the plants were 30-d-old, they were divided into four groups: control, SNPs, NaCl, and NaCl + SNPs. The SNPs and NaCl + SNPs groups were sprayed with 120 mg L^{-1} SNPs solution using a hand-held sprayer bottle until all leaves were wet (using 50 mL per pot) while the control and NaCl groups were sprayed with distilled water. The foliar spray treatment was conducted during 08:00-09:00 h for 4 d. After that salt stress was imposed on the NaCl and NaCl + SNPs groups by removing the flooded water and filled the pots with 150 mM NaCl, while the tap water was refreshed for the control and SNPs groups. The experiment was organized into a completely randomized design (CRD) with four replicates. After the NaCl treatment was imposed for 17 d, leaf greenness and photosynthetic parameters were observed, leaf tissues were sampled for physiological determination, and finally the plants were harvested for the growth measurements. The experiment was conducted during December 2018 to February 2019 with the following weather conditions (maximum temperature 33.95 °C; minimum temperature 20.81 °C; average temperature 27.38 °C, average relative humidity 53.14%; average solar radiation 500 μmol photon m^{-2} s^{-1}).

Growth and biomass. Shoot lengths were measured from the soil surface to the tip of the longest leaf of each plant. The plants were then removed, roots were thoroughly washed to remove soil, patted dry with paper towel, and root length was measured. The shoots and roots were separated, and the fresh weights were recorded. The samples were dried in an oven for 48 h at 70 °C, and then dry weights were measured.

Determination of chlorophyll fluorescence, leaf greenness, and leaf gas exchange parameters

After the salt treatment was imposed for 17 d, measurement of chlorophyll fluorescence of the youngest fully expanded leaf (leaf number 3 from the top) of a randomly selected rice plant in each replicate was conducted in the dark at 20:00 h using a chlorophyll fluorimeter (Handy PEA, Hansatech Instruments, King's Lynn, UK). The maximal quantum efficiency of PSII photochemistry (F_v/F_m) was calculated from minimal fluorescence in the dark-adapted state (F_0) and maximal

fluorescence in the dark-adapted state (F_m), as described by Maxwell and Johnson (2000). On the following day, during 09:00-11:00 h, leaf greenness and leaf gas exchange were measured on the same leaf used for chlorophyll fluorescence measurement. Leaf greenness based on SPAD readings was determined at the top, middle and base of the leaf using SPAD-502 chlorophyll meter (Minolta Corp., Ramsey, New Jersey, USA). Leaf gas exchange was performed using a portable infrared gas exchange analyzer (Li-6400, LI-COR, Lincoln, Nebraska, USA) to determine net photosynthesis rate (P_N), stomatal conductance (g_s), transpiration rate (E). Leaf gas exchange was determined under the following conditions: Chamber temperature 30 °C, CO_2 concentration at 400 ppm, and 30%-70% relative humidity. The photosynthesis photon flux density was maintained at 1500 µmol (photon) m^{-2} s^{-1}.

Preparation of leaf crude extract for determination of biochemical parameters

The same leaves used for data collection on photosynthesis were collected for the determination of biochemical parameters and stored at -80 °C until further processing. Leaf samples (2 g) were ground to a powder with liquid nitrogen in a cold mortar and pestle and then extracted with 6 mL 100 mM potassium phosphate buffer, pH 7.0, containing 1% PVP and 1 mM EDTA. The homogenate was centrifuged at 4500 rpm for 40 min at 4 °C (ROTINA 380 R, Hettich, Tuttlingen, Germany). The crude extract was used to determine H_2O_2, malondialdehyde (MDA) and proline contents, and the activity of antioxidant enzymes.

Determination of MDA content

The MDA content was determined as described by Demiral and Türkan (2005) with modification. The MDA was extracted from 0.2 mL crude extract in 0.8 mL 0.5% thiobarbituric acid (TBA) in 20% trichloroacetic acid (TCA) solution and then boiled for 30 min. The reaction was stopped by placing it on ice for 5 min and centrifuged at 5000 rpm for 10 min. The supernatant was measured at 532 and 600 nm using the microplate reader. The MDA content was calculated using the extinction coefficient of 155 mM cm^{-1} at 532 nm and expressed as nmol g^{-1} FW.

Determination of H_2O_2 content

The level of H_2O_2 from the crude extract was measured using a modified method from Góth (1991); 0.1 mL diluted crude extract (15-fold) was mixed with an equal volume of 32.4 mM ammonium molybdate and then stood for 10 min in dark conditions. The mixture was measured at 405 nm using a microplate reader (EZ Read 2000, Biochrom, Cambridge, UK). The amount of H_2O_2 was calculated using a standard curve of H_2O_2 and expressed as mmol g^{-1} FW.

Determination of proline content

Proline in leaf tissue was determined according to Bates et al. (1973). Proline was extracted from 0.1 mL crude extract by adding 0.1 mL 3% sulfosalicylic acid. Following that, the extract was mixed with 0.2 mL glacial acetic acid and 2.5% ninhydrin. After that, the mixture was boiled for 1 h and stopped the reaction by cooling on ice for 15 min. Then the proline was separated by adding 1 mL toluene at 4 °C. The absorbance of the toluene phase (upper phase) was measured at 520 nm using a spectrophotometer (Spectronic 200, Thermo Scientific, Waltham, Massachusetts, USA). Proline content was calculated and compared with the proline standard curve and expressed as µmol g^{-1} FW.

Determination of activity of antioxidant enzymes

The activity of superoxide dismutase (SOD; EC: 1.15.1.1) was assayed following Beauchamp and Fridovich (1971). The assay mixture (200 µL) consisted of 32 mM phosphate buffer (pH 7.8), 0.4 mM xanthine, 0.5 mM nitro blue tetrazolium chloride (NBT) and the crude extract (20 µg protein). The reaction was started with 3 µL of 20-fold diluted xanthine oxidase and detected rate of reaction was detected at 550 nm in kinetic mode using a microplate reader (SpectraMax M5, Molecular Devices, San Jose, California, USA). The SOD activity was expressed as unit μg^{-1} protein; one unit is the amount of enzyme required to cause 50% inhibition of NBT reduction. For the catalase (CAT; EC: 1.11.1.6) activity, the assay mixture contained 37.5 mM phosphate buffer (pH 7.0), 12.5 mM H_2O_2 and 10 µg protein (Góth, 1991). The decrease in H_2O_2 was detected by measuring the absorbance at 240 nm using the microplate reader in kinetic mode. Enzyme activity is compared with H_2O_2 standard curve and expressed as nmol H_2O_2 oxidized min^{-1} μg^{-1} protein. For ascorbate peroxidase (APX; EC: 1.11.1.11), the activity was assayed following the method of Nakano and Asada (1987). The crude extract (10 µg protein) was mixed with 0.1 mL 100 mM phosphate buffer (pH 7.0) and 40 µL 5 mM ascorbic acid. Afterwards, a reaction was started by adding

35 µL 20 mM H_2O_2 and then monitored the reaction at 290 nm using a microplate reader in kinetic mode. Enzyme activity is compared with ascorbic acid standard curve and expressed as µg ascorbate oxidized min^{-1} $µg^{-1}$ protein. The activity of peroxidase (POX; EC: 1.11.1.7) was assayed as described by Chance and Maehly (1955). The reaction mixture contained 3 µg protein, 38 mM phosphate buffer (pH 6.0) and 30 mM guaiacol. Then a reaction was started by adding 50 µL 20 mM H_2O_2 in 0.2 mL total volume. The increased in absorbance was detected at 415 nm using a microplate reader. Enzyme activity is expressed as ΔA_{415} min^{-1} $µg^{-1}$ protein.

Statistical analysis

All data was analyzed using SPSS 17.0 (IBM, Armonk, New York, USA) to test for significant differences between treatments. The results were expressed as the mean ± standard deviation and the data were subjected to ANOVA and Duncan's multiple range test was used to compare means at a significant difference of $P \leq 0.05$.

RESULTS

Characterization of silica nanoparticles

FE-SEM and EDS analysis. The morphological aspects and elemental compositions of the extracted powder during the calcination process were investigated using the FE-SEM and EDS techniques. The SEM image of SNPs is shown in Figure 2a. The structures are agglomerated semi-spherical nano-sized particles with diameters in the range of 60-135 nm upon calcining. This result demonstrates that the SNP particles are relatively homogeneous. Figure 2b shows the EDS spectra of the calcined silica powder. As disclosed in the EDS result, Si and O were found as the base elements. In addition to Si and O, a small amount of Na and Cu is also presented in the EDS spectrum. The content of Si and O atoms was around 52.2 and 27.1 wt%, respectively.

Figure 2. Field emission scanning electron microscope (FESEM) image (a) and energy-dispersive X-ray spectroscopy (EDS) spectrum of silica nanoparticles (b).

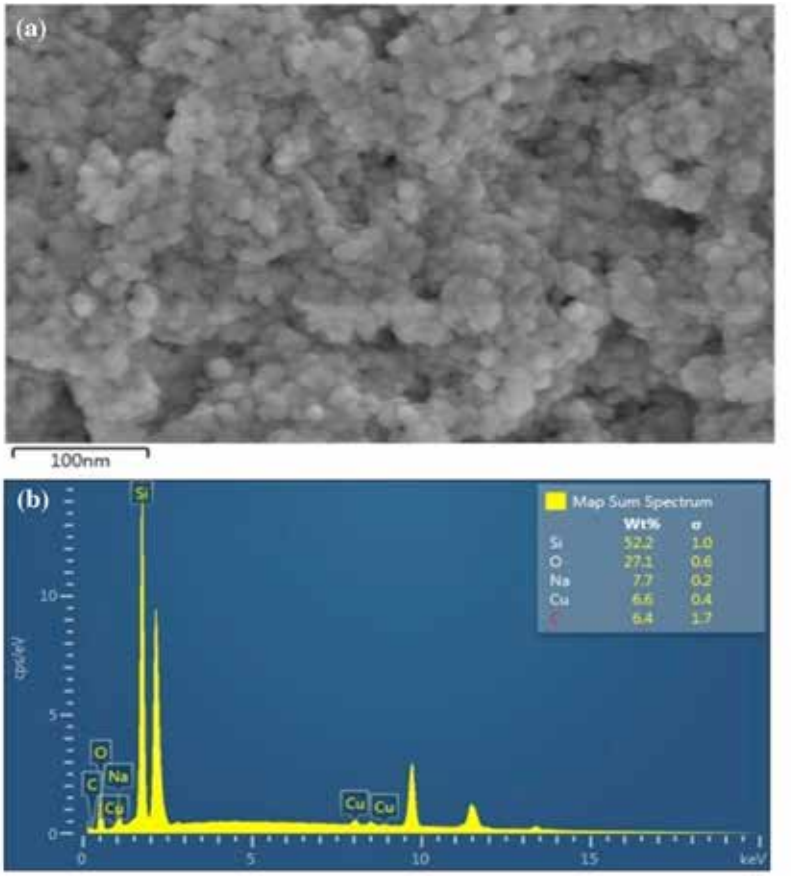

XRD analysis. The synthesized SNPs were characterized by the XRD technique. The XRD patterns of the SNPs obtained from rice husk are shown in Figure 3. As revealed in this figure, a broad peak at 22.9° is seen in the powder diffraction pattern, indicating the formation of the SiO_2 amorphous phase (Downs and Palmer, 1994). The large range of full width at half maximum value in the XRD pattern may also reveal the small size of SiO_2 particles.

FT-IR analysis. The molecular properties of the sample were studied by FT-IR spectroscopy. Figure 4 shows the FT-IR spectrum of the SNPs sample. The broad prominent peak at 1084 cm^{-1} was due to Si-O asymmetric stretching vibration in Si-O-Si bridge band while the other bands at 796 cm^{-1}, 638 cm^{-1} and 614 cm^{-1} were attributed to a network Si-O-Si symmetric bond stretching vibration and a network O-Si-O bond bending modes, respectively.

Effects of foliar spray of SNPs on growth, photosynthesis, and biochemical parameters of rice

Growth parameters. As shown in Figure 5, after rice plants were stressed with 150 mM NaCl for 17 d, plants of all three genotypes showed symptoms of growth reduction, drying of older leaves, and chlorophyll loss of younger leaves. The genotype 'IR29' tended to be the most seriously damaged while 'Pokkali' showed the least symptoms. It was clearly seen that foliar spray of SNPs could alleviate the adverse effects of salt stress. The stressed plants that were pre-treated with SNPs showed lower growth reduction, lower number of dried leaves, and a higher number of green leaves than the NaCl stress plants.

As presented in Table 1, all growth parameters significantly reduced in the salt stress groups compared to the controls. Salt stress resulted in significant reductions in shoot length (SL) of all cultivars, and the application of SNPs alleviated salt stress effects on SL only in 'KDML105' and 'IR29' resulting in significant increases in SL. For all genotypes, root length was more inhibited than shoot length. For root length (RL), when the non-stressed plants were supplemented with SNPs, no beneficial effects on RL were observed. However, for salt-stressed plants, RL of all genotypes was significantly increased compared with that of the salt-stressed plants without SNPs. For biomass, when the non-stressed plants were treated with SNPs, all three genotypes showed significant increase in shoot dry weight (SDW) compared with the controls.

Figure 3. X-Ray diffractometer (XRD) pattern of the extracted silicon after sintering at 900 °C for 7 h.

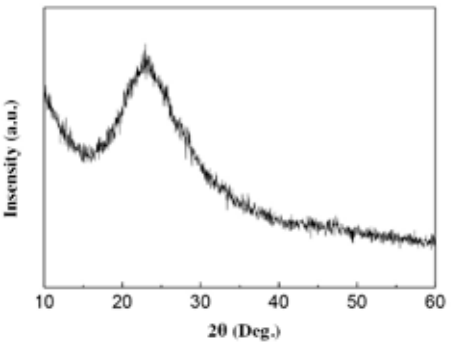

Figure 4. Fourier transform infrared spectroscopy (FT-IR) spectrum of silica nanoparticles.

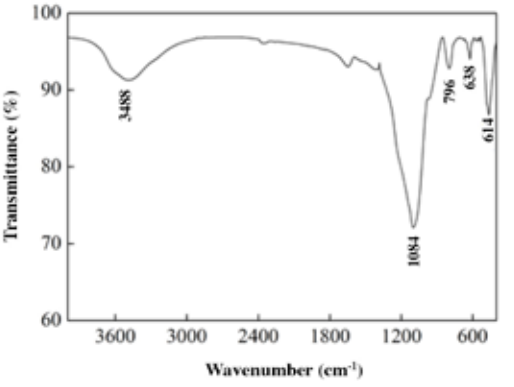

Figure 5. Phenotype of seedlings of three rice cultivars ('IR29', 'KDML105' and 'Pokkali') under control (a), silica nanoparticles (SNPs) (b), 150 mM NaCl (c), and NaCl + SNPs (d) treatments.

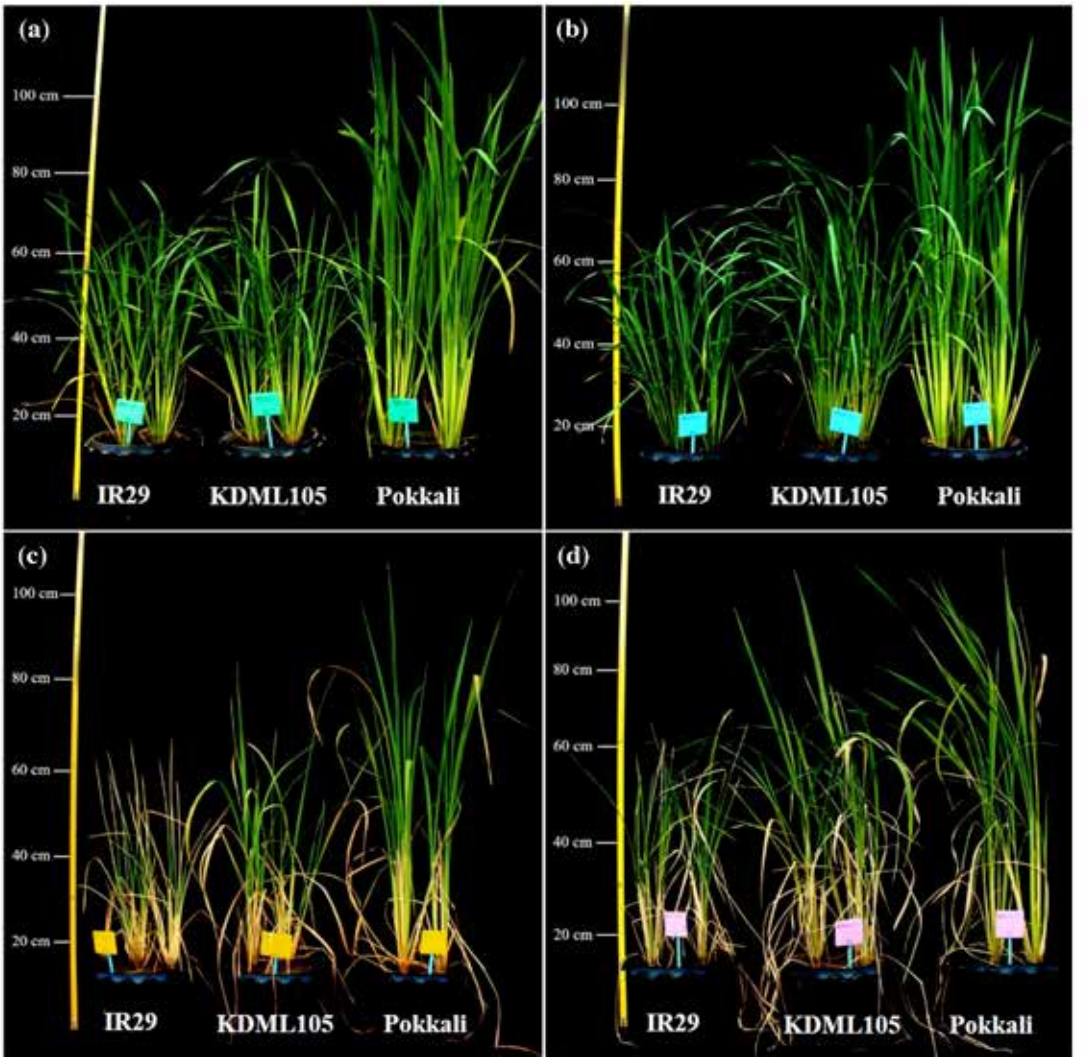

'Pokkali' showed the highest SDW (8.17 g plant^{-1}; 14% increase), followed by 'KDML105' (4.64 g plant^{-1}; 31% increase) and 'IR29' (3.78 g plant^{-1}; 43% increase). In the NaCl-treated conditions, SDW was significantly reduced in 'Pokkali' and 'KDML105'. When the plants were sprayed with SNPs before subjected to salt stress, SDW decreased from control less than in the salt stressed conditions. Salt stress significantly reduced root dry weight (RDW) in all rice genotypes, and foliar spraying of SNPs prior to salt treatment did not show any beneficial effects on RDW.

Changes in leaf gas exchange, chlorophyll fluorescence, and leaf greenness. Under non-stressed conditions, 'IR29' exhibited the highest P_N (31.50 μmol CO_2 m^{-2} s^{-1}), whereas 'Pokkali' had the lowest P_N (25.96 μmol CO_2 m^{-2} s^{-1}). When the non-stressed plants were supplemented with SNPs, nonsignificant changes in P_N were observed in all cultivars (Table 2). Photosynthesis was severely impaired by salt stress causing significant reductions in P_N of all three cultivars with 'IR29' being most inhibited (84% reduction) while P_N of 'KDML105' and 'Pokkali' were reduced by 72% and 57%, respectively. Application of SNPs alleviated the adverse effects of salt stress on photosynthesis resulting in a significant increase in P_N for 'KDML105' (33% increase) and 'IR29' (116% increase), but presented nonsignificant effects for 'Pokkali' (18% increase). As a result of SNPs application, percent reduction in P_N was reduced from 84% to 66% in 'IR29', and from 72% to 63% in 'KDML105'. Responses of stomatal conductance (g_s) to NaCl stress and SNPs applications followed the similar trends as that of the P_N. For transpiration rates (E), the control plants of 'KDML105' and 'IR29' had higher

transpiration rates (9.17 and 9.41 mmol H_2O m^{-2} s^{-1}) than 'Pokkali' (6.83 mmol H_2O m^{-2} s^{-1}). Application of SNPs to the non-stressed plants had negligible effects on transpiration of 'Pokkali' and 'KDML105' but caused a significant increase in E of 'IR29'. Salt stress induced stomatal closure and caused an enormous reduction in E; E in the salt stressed plants were 1.46, 1.06 and 0.72 mmol H_2O m^{-2} s^{-1} in 'Pokkali', 'KDML105' and 'IR29', respectively. Foliar application of SNPs prior to salt exposure led to a significant increase in E (3.20, 2.46 and 2.22 mmol H_2O m^{-2} s^{-1} for 'Pokkali', 'KDML105' and 'IR29', respectively).

The control plants had maximum PSII quantum efficiency (F_v/F_m) of 0.78-0.79 which was close to 0.8, a value documented for plants growing in non-stress conditions (Zhori et al., 2015). Application of SNPs to non-stressed plants had no effects on PSII efficiency (Table 2). NaCl imposed damages to PSII components leading to significantly lower F_v/F_m in all three cultivars (0.74, 0.73 and 0.70 for 'KDML105', 'Pokkali' and 'IR29', respectively). SNPs pre-

Table 1. Effects of foliar application of silica nanoparticles (SNPs) on shoot length (SL), root length (RL), shoot dry weight (SDW), and root dry weight (RDW) of three rice cultivars treated with SNPs, 150 mM NaCl, NaCl + SNPs, and percentage of change compared with the controls.

Cultivars	Treatments	SL		RL		SDW		RDW	
		cm	%	cm	%	g plant^{-1}	%	g plant^{-1}	%
Pokkali	Control	109.75 ± 0.05i	-	36.30 ± 1.19f-h	-	7.20 ± 0.06f	-	6.34 ± 1.28f	-
	SNPs	112.75 ± 3.20j	+3	37.58 ± 0.57h	+4	8.17 ± 0.02g	+1	7.19 ± 0.64g	+13
	NaCl	90.38 ± 1.25g	-18	26.25 ± 0.96bc	-28	4.25 ± 0.02de	-41	1.80 ± 0.20bc	-72
	NaCl+SNPs	90.25 ± 1.26g	-18	30.70 ± 1.76e	-15	4.40 ± 0.04e	-39	2.26 ± 0.23c	-64
KDML105	Control	85.75 ± 0.29f	-	36.88 ± 2.25f-h	-	3.54 ± 0.13c	-	2.38 ± 0.40c	-
	SNPs	94.75 ± 0.50h	+11	37.15 ± 0.83gh	+1	4.64 ± 0.04e	+31	2.34 ± 0.30c	-2
	NaCl	76.25 ± 1.26d	-11	25.63 ± 0.75ab	-31	2.04 ± 0.32a	-42	1.87 ± 0.23bc	-21
	NaCl+SNPs	78.75 ± 0.96e	-8	28.38 ± 1.18d	-23	2.39 ± 0.06ab	-32	1.36 ± 0.14ab	-42
IR29	Control	70.63 ± 0.48c	-	34.90 ± 2.52f	-	2.65 ± 0.13b	-	3.39 ± 0.20e	-
	SNPs	74.88 ± 0.85d	+6	35.25 ± 0.65fg	+1	3.78 ± 0.35cd	+42	3.02 ± 0.25d	-11
	NaCl	58.25 ± 0.65a	-18	23.88 ± 1.31a	-32	2.12 ± 0.16ab	-2	1.15 ± 0.09a	-66
	NaCl+SNPs	62.13 ± 0.85b	-12	27.70 ± 0.62cd	-21	2.24 ± 0.30ab	-1	1.32 ± 0.22ab	-61
Cultivar (C)		**		**		**		**	
Treatments (T)		**		**		**		**	
C×T		**		**		**		**	

*, ** Significant at $P \leq 0.05$ and $P \leq 0.01$ level, respectively; ns: nonsignificant.
The values are the means of four replicates ± SD. Means with different letters are significantly different at $P \leq 0.05$ according to Duncan's multiple range test.

Table 2. Effects of foliar application of silica nanoparticles (SNPs) on net photosynthesis rate (P_N), stomatal conductance (g_s), transpiration rate (E), maximum quantum efficiency of photosystem II (PSII) photochemistry (F_v/F_m), and SPAD readings of leaves of three rice cultivars treated with SNPs, 150 mM NaCl, NaCl + SNPs, and percentage of change compared with the controls.

Cultivars	Treatments	P_N		g_s		E		F_v/F_m		SPAD reading	
		μmol CO_2 m^{-2} s^{-1}	%	mmol m^{-2} s^{-1}	%	mmol m^{-2} s^{-1}	%		%		%
Pokkali	Control	25.96 ± 0.61e	-	0.19 ± 0.01c	-	6.83 ± 0.29e	-	0.78 ± 0.00e	-	38.05 ± 0.44c	-
	SNPs	25.85 ± 0.27e	-0.42	0.25 ± 0.03d	+31	7.10 ± 0.13e	+4	0.78 ± 0.00e	-	38.95 ± 2.24c	+2
	NaCl	11.14 ± 0.26cd	-57	0.03 ± 0.01a	-84	1.46 ± 0.19ab	-79	0.73 ± 0.01ab	-6	30.34 ± 1.06ab	-20
	NaCl+SNPs	13.17 ± 0.56d	-49	0.10 ± 0.01b	-47	3.20 ± 0.15d	-53	0.77 ± 0.00c-e	-1	31.91 ± 0.40b	-16
KDML105	Control	30.88 ± 1.15f	-	0.32 ± 0.03e	-	9.17 ± 0.44f	-	0.79 ± 0.00e	-	38.70 ± 1.04c	-
	SNPs	32.81 ± 1.10fg	+6	0.32 ± 0.03e	0.00	9.58 ± 0.44f	+4	0.78 ± 0.00e	-1	41.25 ± 1.09c	+7
	NaCl	8.60 ± 0.78b	-72	0.02 ± 0.01a	-94	1.06 ± 0.29a	-88	0.74 ± 0.01b-d	-6	29.14 ± 0.71ab	-25
	NaCl+SNPs	11.42 ± 0.73cd	-63	0.07 ± 0.01ab	-78	2.46 ± 0.24cd	-73	0.78 ± 0.02d-e	-1	29.62 ± 0.18ab	-24
IR29	Control	31.50 ± 0.79fg	-	0.32 ± 0.02e	-	9.41 ± 0.36f	-	0.79 ± 0.00e	-	39.18 ± 1.35c	-
	SNPs	33.82 ± 0.97g	+7	0.37 ± 0.03e	+16	10.93 ± 0.35g	+16	0.78 ± 0.00e	-1	38.88 ± 0.76c	-0.77
	NaCl	4.93 ± 0.28a	-84	0.02 ± 0.00a	-94	0.72 ± 0.05a	-92	0.70 ± 0.03a	-11	27.72 ± 0.91a	-29
	NaCl+SNPs	10.64 ± 1.18bc	-66	0.06 ± 0.01ab	-81	2.22 ± 0.29bc	-76	0.74 ± 0.02a-c	-6	30.08 ± 0.79ab	-23
Cultivar (C)		ns		*		ns		ns		ns	
Treatments (T)		**		**		**		**		**	
C×T		**		**		**		**		**	

*, ** Significant at $P \leq 0.05$ and $P \leq 0.01$ level, respectively; ns: nonsignificant.
The values are the means of four replicates ± SD. Means with different letters are significantly different at $P \leq 0.05$ according to Duncan's multiple range test.

treatment to salt-stressed plants alleviated salt-induced damage to PSII leading to significant improvement of F_v/F_m values of 'Pokkali' to 0.77, while the higher values of 'KDMl105' and 'IR29' were not significantly different from the stressed values.

For leaf greenness, all three rice cultivars had similar level of leaf greenness under the control condition (Table 2). SNPs treatment of the non-stressed plants did not alter the SPAD values of all cultivars. Salt stress significantly reduced leaf greenness of all cultivars, and foliar application of SNPs prior to salt treatment did not increase the SPAD values.

Changes in biochemical parameters. Under non-stressed conditions, leaves of all three cultivars had similar amount of malondialdehyde (MDA), and SNPs treatment did not have any significant effects on MDA (Table 3). When subjected to salt stress, significant increases in MDA were observed in all three cultivars. In response to salt stress, 'IR29' produced the highest MDA (19.58 mmol g^{-1} FW; 310% increase compared with control plants), whereas 'Pokkali' had the lowest MDA (15.38 mmol g^{-1} FW; 101% increase compared with control plants). Foliar spraying of SNPs prior to salt treatment did not present any significant effects on the amount of MDA in the salt-stressed plants of all three rice cultivars. 'IR29' still showed the highest MDA (17.89 mmol g^{-1} FW; 274% increase when compared with control plants), whereas 'Pokkali' contained the lowest MDA (14.79 mmol g^{-1} FW; 94% increase compared with control plants).

For hydrogen peroxide content (H_2O_2), under non-stressed conditions, 'KDML105' had the highest H_2O_2 (0.22 mmol g^{-1} FW), whereas 'Pokkali' and 'IR29' produced lower H_2O_2 (0.16 mmol g^{-1} FW). The application of SNPs to the non-stressed plants did not have any effects on H_2O_2 content. Salt stress caused significant increases in H_2O_2 in all three cultivars. Under salt stress, 'Pokkali' produced the highest H_2O_2 (0.51 mmol g^{-1} FW; 219% increase compared with control plants), whereas 'KDML105' showed the lowest H_2O_2 (0.47 mmol g^{-1} FW; 114% increase compared with control plants). Foliar application of SNPs prior to salt exposure resulted in significant decrease in H_2O_2 in 'Pokkali' and 'KDML105'. Under this condition, 'Pokkali' showed the lowest H_2O_2 (0.35 mmol g^{-1} FW; 118.75% increase compared with control plants) while 'IR29' accumulated the highest H_2O_2 (0.45 mmol g^{-1} FW; 181.25% increase compared with control plants).

Under non-stressed conditions, all three cultivars had similar amount of proline in their leaves (0.05-0.06 µmol g^{-1} FW). Foliar application of SNPs to non-stressed plants did not produce any effects on proline content. Salt stress resulted in an enormous increase in proline content, with 'IR29' producing the highest proline (1.02 µmol g^{-1} FW) followed by 'KDML105' (0.91 µmol g^{-1} FW) and 'Pokkali' (0.68 µmol g^{-1} FW). When 'KDML105' and 'IR29' plants were sprayed with SNPs before subjected to salt stress, they produced significantly lower proline than the salt-stressed plants.

For the activity of antioxidant enzymes, it is evident in Table 4 that SNPs in the absence of NaCl stress induced significant increases in APX, POX and CAT in 'Pokkali', POX in 'KDML105' and CAT in 'IR29'. When challenged with NaCl, rice plants generally exhibited increased or stable enzyme activities compared with the controls except for

Table 3. Effects of foliar application of silica nanoparticles (SNPs) on malondialdehyde (MDA), hydrogen peroxide (H_2O_2), and proline of leaves of three rice cultivars treated with SNPs, 150 mM NaCl, NaCl + SNPs, and percentage of change compared with the controls.

Cultivars	Treatments	MDA		H_2O_2		Proline	
		nmol g^{-1} FW	%	mmol g^{-1} FW	%	µmol g^{-1} FW	%
Pokkali	Control	7.64 ± 0.28a	-	0.16 ± 0.01a	-	0.05 ± 0.00a	-
	SNPs	5.22 ± 1.06a	-32	0.17 ± 0.03a	+6	0.04 ± 0.01a	-20
	NaCl	15.38 ± 0.33b	+101	0.51 ± 0.02f	+219	0.68 ± 0.02b	+1260
	NaCl+SNPs	14.79 ± 0.61b	+94	0.35 ± 0.01c	+119	0.70 ± 0.02b	+1300
KDML105	Control	4.46 ± 0.39a	-	0.22 ± 0.02b	-	0.06 ± 0.00a	-
	SNPs	5.17 ± 0.59a	+16	0.19 ± 0.02ab	-14	0.05 ± 0.00a	-17
	NaCl	17.78 ± 0.54bc	+298	0.47 ± 0.01ef	+114	0.91 ± 0.01d	+1417
	NaCl+SNPs	16.88 ± 1.43bc	+278	0.41 ± 0.02d	+84	0.85 ± 0.06c	+1317
IR29	Control	4.78 ± 0.64a	-	0.16 ± 0.02a	-	0.06 ± 0.01a	-
	SNPs	4.77 ± 0.16a	-0.21	0.15 ± 0.01a	-6	0.07 ± 0.00a	+17
	NaCl	19.58 ± 0.87c	+310	0.49 ± 0.01ef	+206	1.02 ± 0.01e	+1600
	NaCl+SNPs	17.89 ± 2.66bc	+274	0.45 ± 0.03de	+181	0.83 ± 0.03c	+1283
Cultivar (C)		ns		ns		**	
Treatments (T)		**		**		**	
C×T		**		**		**	

*, ** Significant at $P \leq 0.05$ and $P \leq 0.01$ level, respectively; ns: nonsignificant.
The values are the means of four replicates ± SD. Means with different letters are significantly different at $P \leq 0.05$ according to Duncan's multiple range test.

Table 4. Effects of foliar application of silica nanoparticles (SNPs) on the activity of superoxide dismutase (SOD), ascorbate peroxidase (APX), peroxidase (POX) and catalase (CAT) of leaves of three rice cultivars treated with SNPs, 150 mM NaCl, NaCl + SNPs, and percentage of change compared with the control.

Cultivars	Treatments	SOD		APX		POX		CAT	
		unit min^{-1} μg^{-1} protein	%	nmol ascorbic acid min^{-1} μg^{-1} protein	%	ΔA_{415} min^{-1} μg^{-1} protein	%	nmol min^{-1} μg^{-1} protein	%
Pokkali	Control	0.182 ± 0.008c-e	-	4.975 ± 0.064e	-	89.95 ± 7.58a	-	318.94 ± 16.24ab	-
	SNPs	0.183 ± 0.005de	+0.6	6.114 ± 0.328gh	+23	248.88 ± 9.87f	+177	507.30 ± 32.11de	+59
	NaCl	0.195 ± 0.001e	+7	5.616 ± 0.086f	+13	129.53 ± 13.19d	+44	558.21 ± 15.38e	+75
	NaCl+SNPs	0.192 ± 0.006e	+6	5.839 ± 0.227fg	+17	108.16 ± 9.53b	+20	458.86 ± 13.18cd	+44
KDML105	Control	0.177 ± 0.010b-d	-	5.690 ± 0.091f	-	117.17 ± 10.21b-d	-	401.69 ± 29.61a-d	-
	SNPs	0.171 ± 0.001bc	-3	3.924 ± 0.278d	-31	270.83 ± 19.60g	+131	434.05 ± 38.65b-d	+8
	NaCl	0.193 ± 0.007e	+9	2.974 ± 0.120c	-48	238.73 ± 6.63ef	+104	353.96 ± 32.56a	-12
	NaCl+SNPs	0.186 ± 0.003de	+5	6.172 ± 0.356h	+8.5	126.22 ± 4.88cd	+8	462.89 ± 33.26cd	+15
IR29	Control	0.166 ± 0.019ab	-	2.692 ± 0.058b	-	122.07 ± 4.90b-d	-	372.52 ± 44.89ab	-
	SNPs	0.157 ± 0.005a	-5	2.535 ± 0.179ab	-5.9	110.38 ± 5.58bc	-10	629.97 ± 19.97f	+69
	NaCl	0.176 ± 0.004b-d	+6	4.038 ± 0.102d	+50	116.15 ± 16.71b-d	-5	398.35 ± 63.40a-c	+7
	NaCl+SNPs	0.157 ± 0.002a	-5	2.355 ± 0.129a	-13	227.96 ± 9.68e	+87	643.26 ± 22.65f	+73
Cultivar (C)		**		**		**		**	
Treatments (T)		**		**		**		**	
C×T		ns		**		**		**	

*, ** Significant at $P \leq 0.05$ and $P \leq 0.01$ level, respectively; ns: nonsignificant.
The values are the means of four replicates ± SD. Means with different letters are significantly different at $P \leq 0.05$ according to Duncan's multiple range test.

'KDML105' which showed a significant reduction in APX and nonsignificant reduction in CAT activity. Response to foliar application of SNPs of the three rice cultivars in the presence of salt stress varied considerably. For salt-stressed plants supplemented with SNPs, significant increases in enzyme activity were observed in CAT (for KDML105' and 'IR29'), POX (for 'IR29'), and APX (for 'KDML105'). For salt stressed 'Pokkali', SNPs caused a reduction in the activity of POX and CAT. Among the four enzymes investigated, NaCl and SNPs resulted in the smallest mostly insignificant changes in SOD activity except for the significant reduction in the SNPs-treated salt stressed plants of 'IR29'.

DISCUSSION

Rice husk is an agricultural waste produced in huge amounts from rice milling process which can pose a threat to the environment. Using rice husk as raw materials for producing valuable silica can contribute to reducing pollution problems caused by uncontrolled burning of rice husk (Dhaneswara et al., 2020). The extraction of nano-silica from rice husk is a simple, cheap, and low-energy method that will benefit both environmental and industrial aspects, with an ever-increasing call for greener and safer technology (Huang et al., 2019). The silica nanoparticles (SNPs) obtained in this study were spherical in morphology and amorphous in nature, as illustrated in Figure 2a. Earlier studies have proven that rice husk SNPs have an amorphous nature (Dhaneswara et al., 2020). The EDS spectrum in Figure 2b shows the presence of Si and O, which confirms the existence of SiO_2, whereas C shows the biological origin of the sample. Si higher energy peak intensity might be because of energy peak overlap due to cross excitation of X-ray signals from different particles (Rades et al., 2014; Ngouangna et al., 2020). From the XRD patterns of the SNPs in Figure 3, the prepared SNPs samples exhibited a peak at $2\theta = 22.9°$ which indicates the presence of SNPs; no other impurities were detected. This XRD pattern is in line with the findings of prior studies (Nayak and Datta, 2021). As shown by the EDS and XRD data, it is plausible to suggest that a modified sol-gel approach is appropriate for synthesizing SNPs from agricultural waste such as rice husk due to a lower cost production compared to the previous works (Mor et al., 2017). FT-IR measurements were performed to identify the chemical functionality of the SNPs as depicted in Figure 4. In general, silica exhibits Si–O stretching and bending vibration bands in the range of 400-1300 cm^{-1} (Rafiee et al., 2012). The spectrum for SNPs included absorption bands at 1084 cm^{-1}, 796 cm^{-1}, and 614 cm^{-1} are assigned to Si–O asymmetric stretching, Si–O–Si symmetric stretching and Si–O–Si bending vibration, respectively, which indicates the existence of silica in the sample. The peak at 3488 cm^{-1} is the vibration peak of –OH bond as the broad peak at 3100-3600 cm^{-1} corresponds to the stretching vibration peak of the –OH bond in the structure water (Martínez et al., 1998).

Exogenous supplementation of Si in the form of soluble silicic acid and SNPs was found to promote plant growth and reduce adverse effects of stress (Siddiqui et al., 2020). In this study, foliar application of SNPs promoted growth, in the absence of stress, by significantly increased shoot dry weight (for 'KDML105 and 'IR29'; Table 1) which was related to the slight increases in P_N (Table 2). Xie et al. (2012) found that foliar application of SNPs at 300 mg L^{-1} significantly increased net photosynthesis rate of the bamboo (*Indocalamus barbatus*) plants in the absence of stress. However, under salt stress, the application of SNPs did not mitigate the salt-induced reduction in SDW (for 'KDML105' and 'IR29') despite the significant increase in P_N (Table 2). The increased P_N was offset by the reduction in leaf area, therefore reducing whole plant photosynthesis and hence biomass (Zhu et al., 2010). Salt stress induced stomatal closure, hence a reduction in g_s which restricted CO_2 diffusion leading to a reduction in P_N. The enhancement of P_N by SNPs under salt stress was explained by the positive effect of SNPs on increasing the stomatal conductance which resulted from the SNP-induced higher plant water status, and the increased activity of carbonic anhydrase which functions in maintaining a constant supply of CO_2 to chloroplast (Siddiqui et al., 2014). Salt-induced reduction in P_N was also related to the toxic effects of sodium ions which damaged structural proteins of photosystem II (Maxwell and Johnson, 2000) causing the impairment of photochemical energy conversion as indicated by the significant reduction in maximal quantum efficiency of PSII photochemistry (F_v/F_m) (Table 2). Foliar application of SNPs was found to mitigate the adverse effects of NaCl and considerably raised the F_v/F_m values (for 'Pokkali' and 'KDML105') to the similar level as that of the control plants. The observations that exogenous SNPs restored stress induced impairment of PSII functions leading to the increments of F_v/F_m were also previously reported in wheat subjected to drought (Maghsoudi et al., 2015).

In response to salt stress, plants synthesized and accumulated high concentrations of proline which acted as an excellent osmolyte involved in osmotic adjustment and maintenance of plant water status (Borzouei et al., 2012; Moukhtari et al., 2020). Proline also provided essential roles under stress as an antioxidant molecule, a metal chelator, a signaling molecule, and a molecule that protects enzyme activity (Hayat et al., 2012). The results in the present study showed that salt-stressed rice plants accumulated 12- to 16-fold proline compared to the control plants, and the more sensitive genotypes ('KDML105' and 'IR29') accumulated more proline than the tolerant one ('Pokkali'). This result was in line with several reports in rice (Kumar et al., 2009; Nounjan et al., 2016; Pamuta et al., 2022). A balance in proline synthesis and degradation is reported to play a critical role during the stress and recovery phase. During salt stress, limiting CO_2 fixation leads to reduced consumption of NADPH and shortage of $NADP^+$ to accept electrons from the electron transport chain, subsequently causing reactive oxygen species (ROS) production because of electron transfer to oxygen. Proline synthesis pathway in the chloroplast utilizes NADPH, regenerates $NADP^+$ which enters the electron transport, thereby reducing ROS production (Signorelli, 2016). During stress recovery, proline converts back to glutamate generating NADH and $FADH_2$ which are utilized to generate ATP in the mitochondria (Moukhtari et al., 2020). The treatment of SNPs, in the present study, leads to a significant reduction in proline indicating that the plants were relieved from stress and started to degrade proline. Abdel-Haliem et al. (2017) investigated the effects of SNPs (average diameter of 10 nm) on salt-stressed pot-grown rice seedlings by directly applying SNPs (50 mL of 150 g L^{-1} SNPs solution) to the pot containing 2 kg soil. These authors also reported the mitigating effects of SNPs that results in the reduction of proline in salt-stressed rice under moderate NaCl stress (100-200 mM).

Salt stress induced an overaccumulation of ROS like superoxide anion, hydroxyl radicals, and H_2O_2, which actively oxidized essential macromolecules including membrane lipids and proteins leading to membrane damage, protein degradation, alteration in metabolism, and ultimately cell death (Miller et al., 2010). In the present study, NaCl imposed high levels of stress to rice plants as indicated by 2- to 3-fold increase in H_2O_2 as compared to the controls, and SNPs considerably reduced the amount of harmful ROS especially in the case of 'Pokkali' and 'KDML105' (Table 3). The alleviating effects of SNPs on the reduction of H_2O_2 production in salt-stressed rice plants were previously reported by Abdel-Haliem et al. (2017) when the plants were challenged with moderate salt levels (100-200 mM NaCl). One of the most damaging actions of ROS involves an attack on polyunsaturated lipids in the membrane through an oxidative chain reaction, lipid peroxidation. Lipid peroxidation produces several by-products including MDA which is widely used as an indicator for the level of lipid peroxidation. Rice plants under salt stress produced 2- to 4- fold increase in MDA, but SNPs pretreatment did not significantly reduce the MDA content (Table 3). Similar results were reported in Abdel-Haliem et al. (2017) that SNPs resulted in minimal reduction in MDA in salt-stressed rice plants. In contrast, Siddiqui et al. (2014) found that SNPs (0.5 to 7.5 g L^{-1}) applied simultaneously with NaCl (120 mM) to squash (*Cucurbita pepo* L.) seedlings

effectively reduced the amount of MDA. Therefore, the effectiveness of SNPs on modifying or mitigating physiological parameters of salt-stressed plants depends on the plant species, the developmental stage, the concentrations of NaCl, and the application method and concentrations of SNPs.

One of the most important strategies of plants to alleviate adverse effects of salt stress is to develop intricated non-enzymatic and enzymatic antioxidant systems to destroy ROS (Miller et al., 2010). In this study, SNPs invoked varying patterns of responses in relation to activities of antioxidant enzymes in different rice cultivars under salt stress. For 'KDML105' and 'Pokkali', lower contents of H_2O_2 in the salt stressed plants treated with SNPs compared to the salt stressed plants were due to high activities of CAT and APX, while 'IR29' displayed prominent activities of CAT and POX. Upregulation of CAT and POX activities in response to SNPs was previously reported in rice 'Skha 1' (Abdel-Haliem et al., 2017) and squash (Siddiqui et al., 2014). For the salt tolerant 'Pokkali', the lower level of CAT activity in the SNPs-treated salt stress plants indicated lower level of stress and less regulation of H_2O_2. This type of response was previously reported in rice 'Dongjin' (Kim et al., 2013). Kim et al. (2017) reported that Si-supplemented plants showed enhanced resistance to abiotic stress through lowering ROS production by enhancing activity of antioxidant enzymes (particularly CAT) which converts H_2O_2 to H_2O, thereby decreasing MDA and oxidative damages.

Both commercial SiO_2 fertilizer and SNPs were reported to be beneficial for rice under salt stress, but SNPs could be applied at millimolar ranges as foliar spray which was considerably lower than Si fertilizer dosage (Liu et al., 2009), therefore reducing the cost of rice production in the areas of problem soils. In this study, foliar application of low concentration of SNPs alleviated adverse effects of NaCl by modulating many physiological and biochemical processes in rice. The mitigating effects of SNPs included (1) the protection of damage to PSII and enhancement of stomatal conductance resulting in significant improvement of net photosynthesis rates, (2) the reduction in ROS content through enhanced activity of antioxidant enzymes leading to reduced levels of cellular stress, and (3) reduction in proline synthesis. Since SNP-mediated response varies with size, shape, physicochemical properties (Rastogi et al., 2019), these variables should be explored in future experiments to determine the most effective ways of using SNPs to reduce deleterious effects of salt on rice.

CONCLUSIONS

This study was conducted to produce environmentally friendly and cost-effective silica nanoparticles (SNPs) from rice husk, a voluminous agricultural waste. The SNPs produced were semi-spherical nano-sized porous silica with an amorphous nature. The foliar application of SNPs to rice plants reduced salt stress by modulating important physiological and biochemical processes including enhancing photosynthesis performance, regulating antioxidant enzyme activities, and reducing toxic reactive oxygen species and proline.

ACKNOWLEDGEMENTS

This research was funded by Research Fund for Supporting Lecturer to Admit High Potential Students to Study and Research on His Expert Program Year 2015, Graduate School, Khon Kaen University (KKU), and KKU Research and Graduate Affairs for funding the Research Program RP64-11-001. The authors also acknowledge the grant from the National Research Council of Thailand (NRCT) through the Senior Research Scholar Project of Prof. Dr. Piyada Theerakulpisut (Project N° NRCT813/2563). The authors are grateful for the Faculty of Agriculture, Khon Kaen University for providing the greenhouse space.

REFERENCES

Abdel-Haliem, M.E., Hegazy, H.S., Hassan, N.S., and Naguib, D.M. 2017. Effect of silica ions and nano silica on rice plants under salinity stress. Ecological Engineering 99:282-289. doi.org/10.1016/j.ecoleng.2016.11.060.

Agarie, S., Hanaoka, N., Ueno, O., Miyazaki, A., Kubota, F., Agata, W., et al. 1998. Effects of silicon on tolerance to water deficit and heat stress in rice plants (*Oryza sativa* L.), monitored by electrolyte leakage. Plant Production Science 1:96-103. doi.org/10.1626/pps.1.96.

Bates, L.S., Waldren, R.P., and Teare, I.D. 1973. Rapid determination of free proline for water-stress studies. Plant and Soil 39(1):205-207. doi.org/10.1007/BF00018060.
Beauchamp, C., and Fridovich, I. 1971. Superoxide dismutase: improved assays and an assay applicable to acrylamide gels. Analytical Biochemistry 44(1):276-287. doi.org/10.1016/0003-2697(71)90370-8.
Borzouei, A., Kafi, M., Akbari-Ghogdi, E., and Mousavi-Shalmani, M. 2012. Long term salinity stress in relation to lipid peroxidation, superoxide dismutase activity and proline content of salt sensitive and salt-tolerant wheat cultivars. Chilean Journal of Agricultural Research 72:476-482. doi:10.4067/S0718-58392012000400003.
Chance, B., and Maehly, A.C. 1955. Assay of catalase and peroxidase. Methods in Enzymology 2:764-775. doi:10.1016/S0076-6879(55)02300-8.
Cuong, T.X., Ullah, H., Datta, A., and Hanh, T.C. 2017. Effects of silicon-based fertilizer on growth, yield and nutrient uptake of rice in tropical zone of Vietnam. Rice Science 24:283-290. doi:10.1016/j.rsci.2017.06.002.
Demiral, T., and Türkan, I. 2005. Comparative lipid peroxidation, antioxidant defense systems and proline content in roots of two rice cultivars differing in salt tolerance. Environmental and Experimental Botany 53(3):247-257. doi:10.1016/j.envexpbot.2004.03.017.
Dhaneswara, D., Fatriansyah, J.F., Situmorang, F.W., and Haqoh, A.N. 2020. Synthesis of amorphous silica from rice husk ash: comparing HCl and CH_3COOH acidification methods and various alkaline concentrations. Synthesis 11(1):200-208. doi:10.14716/ijtech.v11i1.3335.
Downs, R.T., and Palmer, D.C. 1994. The pressure behavior of α cristobalite. American Mineralogist 79(1-2):9-14.
Farid, M., Nasaruddin, Anshori, M.F., Musa, Y., Iswoyo, H., and Sakinah, A.I. 2021. Interaction of rice salinity screening in germination and seedling phase through selection index based on principal components. Chilean Journal of Agricultural Research 81:368-377. doi:10.4067/S0718-58392021000300368.
Félix Alvarez, R.D., Prado, R.D., Felisberto, G., Fernandes Deus, A.C., and Lima de Oliveira, R.L. 2018. Effects of soluble silicate and nanosilica application on rice nutrition in an Oxisol. Pedosphere 28(4):597-606. doi:10.1016/S1002-0160(18)60035-9.
Góth, L. 1991. A simple method for determination of serum catalase activity and revision of reference range. Clinica Chimica Acta 196:143-152. doi:10.1016/0009-8981(91)90067-M.
Hayat, S., Hayat, Q., Alyemeni, M.N., Wani, A.S., Pichtel, J., and Ahmad, A. 2012. Role of proline under changing environments: a review. Plant Signaling and Behavior 7(11):1456-1466. doi:10.4161/psb.21949.
Huang, S.S., Tung, M.T., Huynh, C.D., Hwang, B.J., Bieker, P.M., Fang, C.C., et al. 2019. Engineering rice husk into a high-performance electrode material through an ecofriendly process and assessing its application for lithium-ion sulfur batteries. ACS Sustainable Chemistry and Engineering 7(8):7851-7861. doi:10.1021/acssuschemeng.9b00092.
Kanawapee, N., Sanitchon, J., Lontom, W., and Threerakulpisut, P. 2012. Evaluation of salt tolerance at the seedling stage in rice genotypes by growth performance, ion accumulation, proline, and chlorophyll content. Plant and Soil 358:235-249. doi:10.1007/s11104-012-1179-6.
Kim, Y., Khan, A., Waqas, M., and Lee, I. 2017. Silicon regulates antioxidant activities of crop plants under abiotic-induced oxidative stress: A review. Frontiers in Plant Science 8:510. doi:10.3389/fpls.2017.00510.
Kim, Y., Khan, A., Waqas, M., Shim, J.K., Kim, D., Lee, K., et al. 2013. Silicon application to rice root zone influenced the phytohormonal and antioxidant responses under salinity stress. Journal of Plant Growth Regulation 33:137-149. doi:10.1007/s00344-013-9356-2.
Kumar, V., Shriram, V., Kavi Kishor, P.B., Jawali, N., and Shitole, M.G. 2009. Enhanced proline accumulation and salt stress tolerance of transgenic indica rice by over-expressing P5CSF129A gene. Plant Biotechnology Reports 4:37-48. doi:10.1007/s11816-009-0118-3.
Liu, C., Li, F., Luo, C., Liu, X.M., Wang, S., Liu, T., et al. 2009. Foliar application of two silica sols reduced cadmium accumulation in rice grains. Journal of Hazardous Materials 161(2-3):1466-1472. doi:10.1016/j.jhazmat.2008.04.116.
Luyckx, M., Hausman, J., Lutts, S., and Guerriero, G. 2017. Silicon and plants: Current knowledge and technological perspectives. Frontiers in Plant Science 8:411. doi:10.3389/fpls.2017.00411.
Ma, J.F., Tamai, K., Ichii M., and Wu, G.F. 2002. A rice mutant defective in Si uptake. Plant Physiology 130:2111-2117. doi:10.1104/pp.010348.
Maghsoudi, K., Emam, Y., and Ashraf, M. 2015. Influence of foliar application of silicon on chlorophyll fluorescence, photosynthetic pigments, and growth in water-stressed wheat cultivars differing in drought tolerance. Turkish Journal of Botany 39:625-634. doi:10.3906/bot-1407-11.
Martínez, J.R., Ruiz, F., Vorobiev, Y.V., Pérez-Robles, F., and González-Hernández, J. 1998. Infrared spectroscopy analysis of the local atomic structure in silica prepared by sol-gel. The Journal of Chemical Physics 109(17):7511-7514. doi:10.1063/1.477374.
Maxwell, K., and Johnson, G.N. 2000. Chlorophyll fluorescence: a practical guide. Journal of Experimental Botany 51:659-668. doi:10.1093/jexbot/51.345.659.
Miller, G., Suzuki, N., Ciftci-Yilmaz, S., and Mittler, R. 2010. Reactive oxygen species homeostasis and signalling during drought and salinity stresses. Plant Cell and Environment 33:453-467. doi:10.1111/j.1365-3040.2009.02041.x.

Mor, S., Manchanda, C.K., Kansal, S.K., and Ravindra, K. 2017. Nanosilica extraction from processed agricultural residue using green technology. Journal of Cleaner Production 143:1284-1290. doi:10.1016/j.jclepro.2016.11.142.

Moukhtari, A.E., Cabassa-Hourton, C., Farissi, M., and Savouré, A. 2020. How does proline treatment promote salt stress tolerance during crop plant development? Frontiers in Plant Science 11:1127. doi:10.3389/fpls.2020.01127.

Nakano, Y., and Asada, K. 1987. Purification of ascorbate peroxidase in spinach chloroplasts; its inactivation in ascorbate-depleted medium and reactivation by monodehydroascorbate radical. Plant and Cell Physiology 28(1):131-140. doi:10.1093/oxfordjournals.pcp.a077268.

Nayak, P.P., and Datta, A.K. 2021. Synthesis of SiO_2-nanoparticles from rice husk ash and its comparison with commercial amorphous silica through material characterization. Silicon 13(4):1209-1214. doi:10.1007/s12633-020-00509-y.

Ngouangna, E.N., Manan, M.A., Oseh, J.O., Norddin, M.N.A.M., Agi, A., and Gbadamosi, A.O. 2020. Influence of (3-aminopropyl) triethoxysilane on silica nanoparticle for enhanced oil recovery. Journal of Molecular Liquids 315:113740. doi:10.1016/j.molliq.2020.113740.

Nounjan, N., Siangliw, J.L., Toojinda, T., Chadchawan, S., and Theerakulpisut, P. 2016. Salt-responsive mechanisms in chromosome segment substitution lines of rice (*Oryza sativa* L. cv. KDML105). Plant Physiology and Biochemistry 103:96-105. doi:10.1016/j.plaphy.2016.02.038.

Pal, N., Lee, J.H., and Cho, E.B. 2020. Recent trends in morphology-controlled synthesis and application of mesoporous silica nanoparticles. Nanomaterials 10(11):2122. doi:10.3390/nano10112122.

Pamuta, D., Siangliw, M., Sanitchon, J., Pengrat, J., Siangliw, J.L., Toojinda, T., et al. 2022. Physio-biochemical traits in improved KDML105 rice (*Oryza sativa* L.) lines containing drought and salt tolerance gene under drought and salt stress. Chilean Journal of Agricultural Research 82:97-110. doi:10.4067/S0718-58392022000100097.

Rades, S., Hodoroaba, V.D., Salge, T., Wirth, T., Lobera, M.P., Labrador, R.H., et al. 2014. High-resolution imaging with SEM/T-SEM, EDX and SAM as a combined methodical approach for morphological and elemental analyses of single engineered nanoparticles. RSC Advances 4(91):49577-49587. doi:10.1039/C4RA05092D.

Rafiee, E., Shahebrahimi, S., Feyzi, M., and Shaterzadeh, M. 2012. Optimization of synthesis and characterization of nanosilica produced from rice husk (a common waste material). International Nano Letters 2(1):1-8. doi:10.1186/2228-5326-2-29.

Rastogi, A., Tripathi. D.K., Yadav, S., Chauhan, D.K., Živčák, M., Ghorbanpour, M., et al. 2019. Application of silicon nanoparticles in agriculture. 3 Biotech 9(3):90. doi:10.1007/s13205-019-1626-7.

Savant, N.K., Snyder, G.H., and Datnoff, L.E. 1996. Silicon management and sustainable rice production, Advances in Agronomy 58:151-199. doi:10.1016/S0065-2113(08)60255-2.

Siddiqui, H., Ahmed, K.B.M., Sami, F., and Hayat, S. 2020. Silicon nanoparticles and plants: Current knowledge and future perspectives. p. 129-142. In Hayat, S., Pichtel, J., Faizan, M., and Fariduddin, Q. (eds.) Sustainable agriculture reviews 41. Nanotechnology for plant growth and development. Springer, Cham, Switzerland. doi:10.1007/978-3-030-33996-8_7.

Siddiqui, M.H., Al-Whaibi, M.H., Faisal, M., and Al Sahli, A.A. 2014. Nano-silicon dioxide mitigates the adverse effects of salt stress on *Cucurbita pepo* L. Environmental Toxicology and Chemistry 33(11):2429-2437. doi:10.1002/etc.2697.

Signorelli, S. 2016. The fermentation analogy: a point of view for understanding the intriguing role of proline accumulation in stressed plants. Frontiers in Plant Science 7:1339. doi:10.3389/fpls.2016.01339.

Xie, Y., Li, B., Tao, G., Zhang, Q., and Zhang, C. 2012. Effects of nano-silicon dioxide on photosynthetic fluorescence characteristics of *Indocalamus barbatus* McClure. Journal of Nanjing Forestry University (Natural Sciences Edition) 36(2):59-63. http://njlydxxb.periodicals.net.cn/de.

Zargar, S.M., Mahajan, R., Bhat, J.A., Nazir, M., and Deshmukh, R. 2019. Role of silicon in plant stress tolerance: opportunities to achieve a sustainable cropping system. 3 Biotech 9(3):73. doi:10.1007/s13205-019-1613-z.

Zhori, A., Meco, M., Brandl, H., and Bachofen, R. 2015. In situ chlorophyll fluorescence kinetics as a tool to quantify effects on photosynthesis in *Euphorbia cyparissias* by a parasitic infection of the rust fungus *Uromyces pisi*. BMC Research Notes 8:698. doi.org/10.1186/s13104-015-1681-z.

Zhu, Y., and Gong, H. 2014. Beneficial effects of silicon on salt and drought tolerance in plants. Agronomy and Sustainable Development 34:455-472. doi:10.1007/s13593-013-0194-1.

Zhu, X.G., Long, S., and Ort, D.R. 2010. Improving photosynthetic efficiency for greater yield. Annual Review of Plant Biology 61:235-261. doi:10.1146/annurev-arplant-042809-112206.